

Recovering AVA from acoustic FWI image gathers: a North Sea case study

S. Dong¹, F. Gao¹, Y. He¹, J. Sheng¹, F. Liu¹, B. Wang¹, C. Calderon¹

¹ TGS

Summary

Acoustic FWI has been widely applied in seismic work programs. The normal derivative of the FWI velocity model, which is known as the FWI Image, has been shown to provide a highly interpretable product within a fraction of the time of conventional processing. FWI images are widely used to image reservoirs in a variety of settings, from simple stratigraphic traps to sub-salt exploration targets. However, failing to take into account the elastic effects in acoustic FWI can result in a smeared FWI image caused by amplitude and phase distortions. Elastic FWI can intrinsically solve for this but it requires not only much more computational cost but also accurate elastic models. Alternatively, a multi-angle acoustic FWI can be applied to handle the elastic AVO effects. The input data is first decomposed to different angle ranges, then acoustic FWI is applied to each of them separately, and FWI Image angle gathers are generated. With this approach, high resolution features are maintained in each angle gather. The elastic AVO parameters can then be accurately extracted from the FWI Image angle gathers term applied. This paper discusses the successful application of this approach to an OBC data set from the North Sea.

Recovering AVA from acoustic FWI image gathers: a North Sea case study

Introduction

Acoustic Full-waveform inversion (FWI) is now routinely applied to most seismic processing projects. The use of FWI has resulted in greatly improved velocity model building in terms of both an accurate representation of the subsurface but also achieved this in significantly shorter time frames relative to conventional model building approaches. FWI derived models are generated from data with minimal processing and with the advent of FWI imaging, the scope of FWI applications has been extended further into the imaging landscape (Kalinicheva et al., 2020; Wang, et al., 2021). Compared to a conventional RTM, FWI image is equivalent to a least-squares solution, offering less migration artifacts, better illumination, and higher signal-to-noise ratio. As an FWI image is obtained from the full wavefield data, including transmitted waves, primaries, and multiples, it often provides additional structural information. This allows it to better honour geologic structures, especially in highly complex areas.

Acoustic FWI imaging faces challenges in areas with strong elastic effects, which may result in amplitude and phase distortion with offset increase, causing discrepancies between the observed and synthetic data. Significant research has been focused on this problem. An Elastic FWI algorithm is proposed to overcome the deficiencies of the acoustic modelling process (Liu et al., 2024). Elastic FWI images show considerable improvements in event focusing, structural continuity, and higher signal-to-noise ratio around and beneath salt boundaries. However, acoustic FWI is still the dominant applications of FWI technology in the oil and gas industry, predominantly because of the efficiencies when deriving a high frequency model.

Significant efforts have been devoted to address the elastic impact on acoustic FWI. Gao et al. (2023) attempted to correct the phase reversals caused by elastic AVO effects by decomposing the input data in different angle ranges. This approach yielded high resolution results for a subset of the input data within a certain angle range. Warner et al. (2022) proposed a method to build true amplitude acoustic FWI image angle gathers and extract elastic AVA parameters from them.

In this paper, we apply 3D acoustic dynamic matching FWI to a real dataset from the North Sea in angle domain, where the reservoir presents a class 2p amplitude variation with offset. After a proper amplitude mapping, the correct amplitude vs offset (AVO) is recovered in the resultant FWI image angle gathers.

Method

To generate true amplitude acoustic FWI image gathers, the kinematic and dynamic contributions to FWI are treated separately in a two-stage process. The first phase focuses on kinematic matching to produce a smooth velocity model where the acoustic Dynamic Matching FWI (DMFWI) is applied (Mao et al., 2019) to the full-offset data in lower frequency bands (<20Hz).

In the second phase, the inversion concentrates on recovering the dynamic properties of high-resolution model. The input data are divided into separate incident angle groups (10 degrees bands). Within each group, the reflection angle variation is small, the amplitude and phase are rather consistent with limited discrepancy and amplitude matching is now feasible. In this stage, an objective function that honours the amplitude of the field data is employed in the inversion. An FWI image is then obtained by applying directional differentiation to the inverted P-wave velocity model of each angle range. These FWI images contain AVA information, but in a different form compared to the conventional data. An amplitude mapping of the FWI image gathers is required and is obtained using a modification of the Zoeppritz equations based on the acoustic FWI model parameters that we have determined. In this way, we transform the FWI-AVA result into a conventional AVA result (Warner et al., 2022).

Field data example

The seismic data used in this study is acquired in the North Sea. It is comprised of 30 cables of ocean bottom data acquired in two swaths. The nominal shot carpet spacing of 37.5m and the notional receiver interval of 25m along the cable, with cables separated by 262.5m. The largest offset available is around 8km from the raw hydrophone data and 6km in the processed up-down deconvolved data.

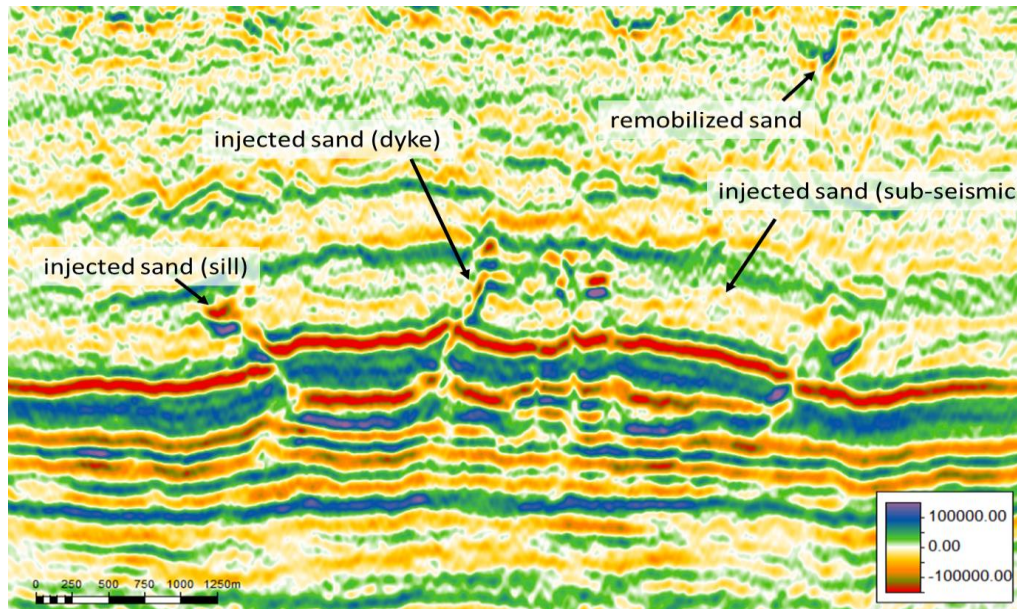


Figure 1 A section showing the geological setting at the imaging target.

The key intervals of interest are shown in Figure 1, where the reservoir zone is imbedded with thin steeply-dipping dykes (e.g., injected sand). AVO anomalies are observed in the reservoir zone as shown in the prestack CMP gather in Figure 2a. There is a clear polarity change as offset increases. Using the model parameters derived from well logs (Figure 2b), the synthetic reflection coefficient shows clear class 2p AVO behaviour (Figure 2c). An acoustic synthetic CMP gather (Figure 2d) shows apparent mismatch of phase versus offset to the real data (Figure 2a), which poses a great challenge for conventional acoustic FWI workflow to recover the proper model parameters.

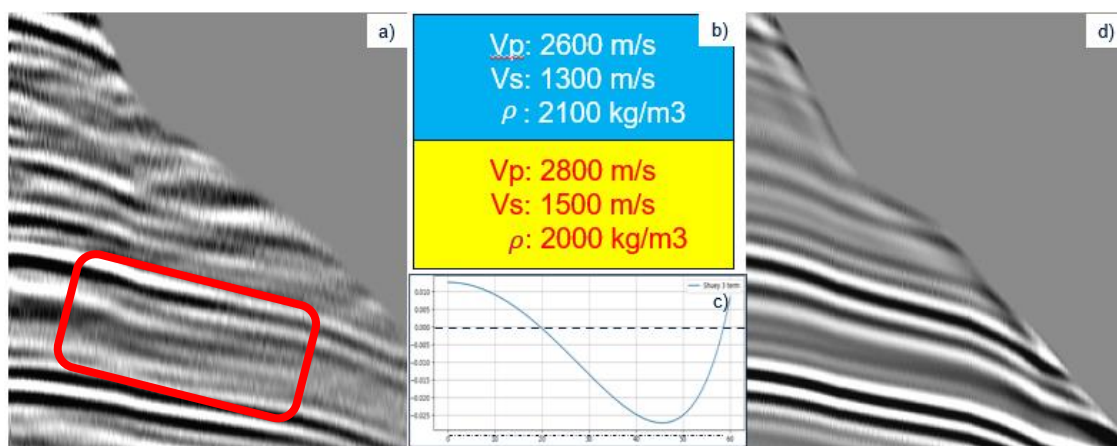


Figure 2: a) A CMP gather near the reservoir showing amplitude and phase distortion as offset increases; b) the model parameters decoded from 3 well logs above and below the reservoir reflector; c) the analytical reflection coefficient computed using Shuey's equation; d) the corresponded acoustic synthetic data.

We applied the acoustic FWI angle gather workflow to this data. Acoustic DMFWI is first applied on the full-offset data in several frequency bands, starting at 3Hz and gradually increasing to 18 Hz. We

focused on building a kinematically correct velocity model to get broad agreement between the observed and model data. The input data were then divided into five angle groups (0-10, 10-20, 20-30, 30-40, and 40-50 degrees) such that the traces in each group cover approximately the same range of reflection angle. An acoustic FWI with an objective function honouring the field data amplitude is performed to each group of the input data, starting at a frequency of 18 Hz and gradually increasing to 50 Hz.

The final FWI velocities and corresponding FWI images for two angle groups (0-10 degrees and 30-40 degrees) are shown in Figure 3. Comparing the two inverted velocity models on the left, the near angle velocity (Figure 3a) has lower resolution than the larger angle range (Figure 3c) at the reservoir level indicated by the arrow, note the polarities are even opposite. These differences can be more clearly observed in the corresponding FWI images. As predicted by the analytical reflection coefficients in Figure 2c, the FWI image for the near angle (0-10 degrees) (Figure 3b) has different polarity to that of far angle (30-40 degrees) FWI image (Figure 3d).

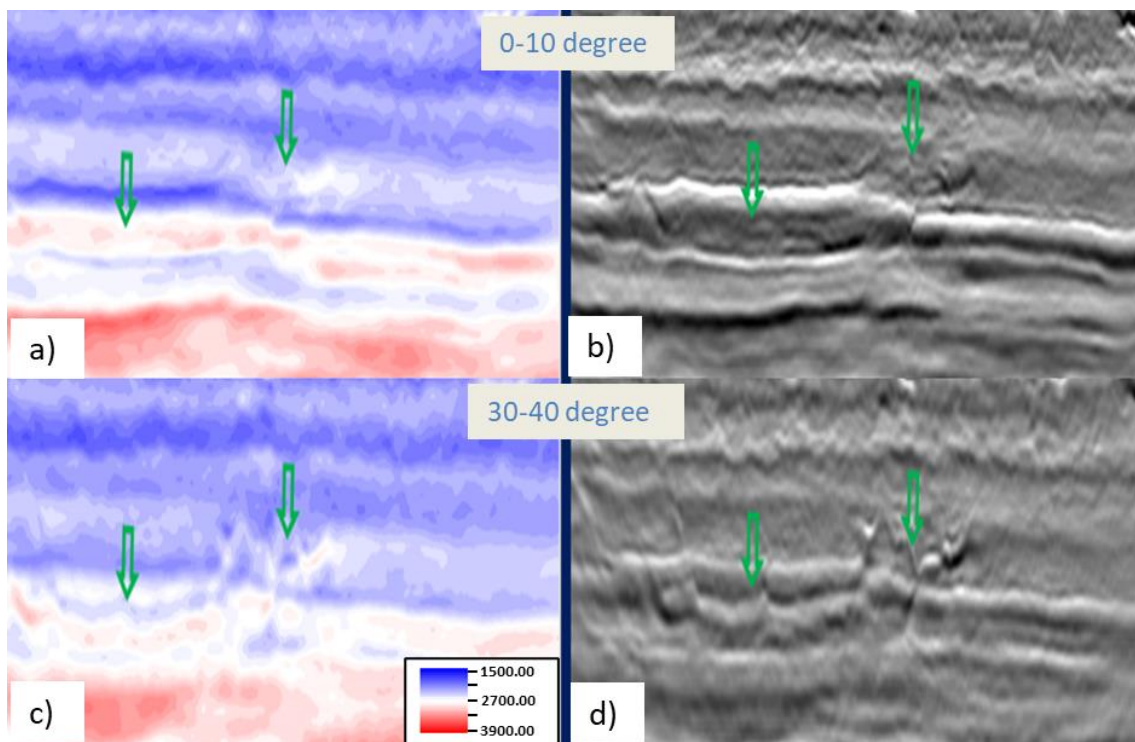


Figure 3: The final FWI velocity model for: **a)** near angle (0-10 degrees), **c)** far angle (30-40 degrees). The final FWI images for: **b)** near angle (0-10 degrees), **d)** far angle (30-40 degrees).

To validate the results, we compared the derived acoustic FWI image angle gather (Figure 4a) with the angle gather from Kirchhoff migration (Figure 4b) at the well location. The red arrows show the key event of focus, both angle gathers exhibit the similar amplitude variation trend versus angle: from positive in near angle to negative in far angle. This observation agrees with class 2p AVO behaviour predicted from the well log. Figure 4c shows a zoomed view of the event at the reservoir near the well location along which the AVO regression shown is extracted and plotted in Figure 4d together with the theoretical AVO curve generated from Shuey's approximation using the parameters decoded from the well log. The degree of correlation shown between the theoretical and computed curves clearly demonstrate the validity of the approach.

Conclusions

We have demonstrated the ability to extract AVO properties from acoustic FWI image gathers on OBC field data using the workflow: splitting the input data into different angle ranges and inverting each subset individually followed by correcting the amplitude variation with a deterministic correction. The approach requires no shear wave velocity nor other information beyond conventional acoustic FWI

requirements. This method enables high resolution and reliable AVO information directly from acoustic FWI imaging.

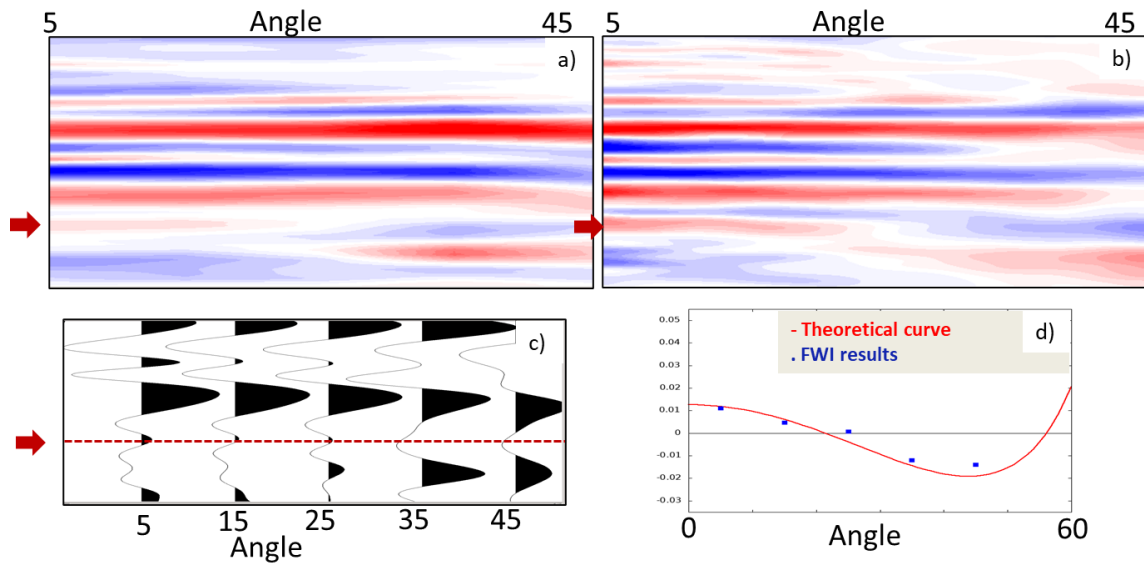


Figure 4 a) A FWI image angle gather at the well location. b) The Kirchhoff offset gather in the same location. c) Zoomed in view of the FWI image angle gather in the reservoir area. d) The amplitude of the FWI image overlaid with the theoretical AVO curve in the reservoir area.

Acknowledgements

We thank AkerBP and Vår Energi ASA for the permission to use and publish the real data examples. We also want to thank TGS management team, Josef Heim, Paul Farmer and Adriana Citlali Ramirez, for their support and permission to publish this work.

References

- Gao, F., Dong, S., He, Y., Sheng, J., Liu, F., Wang, B., Calderon, C., Ivanov, Y., Marcy, F.D., and Aaker, O.E. [2023]. High resolution imaging by dynamic matching FWI in the presence of AVO effects. SEG Technical Program Expanded Abstracts.
- Kalinicheva, T., Warner, M., and Mancini, F. [2020] Full-bandwidth FWI: SEG Technical Program Expanded Abstracts.
- Liu, F., Macesanu, C., Hu, H., Gao, F., Zhan, G., Huang Y., Sheng J., He, Y., Calderon C. and Wang B. [2024] Enhance P wave imaging using elastic dynamic matching FWI, 2024 EAGE
- Mao, J., Sheng, J., and Hilburn, G. [2019] Phase only reflection full-waveform inversion for high resolution model update. 89th Annual International Meeting, SEG, Expanded Abstracts, 1305-1309.
- Wang, B., Y. He, J. Mao, F. Liu, F. Hao, Y. Huang, M. Perz and S. Michell, 2021, Inversion-based imaging: from LSRTM to FWI imaging: First Break, Vol. 39
- Warner, M., Armitage, J., Umpleby, A., Shah, N., Debens, H., and Mancini, F. [2022] Full-elastic AVA extraction using acoustic FWI, Second International Meeting for Allied Geoscience & Energy.